Solid State Communications, Vol. 65, No. 9, pp. 1039–1044, 1988.
Printed in Great Britain.

0038–1098/88 $3.00 + .00
Pergamon Press plc

PARAMAGNETIC RESONANCE OF A Se–Al COMPLEX IN SILICON

A.B. van Oosten and C.A.J. Ammerlaan

Natuurkundig Laboratorium der Universiteit van Amsterdam, Valckenierstraat 65, 1018 XE Amsterdam,
The Netherlands

(*Received* 21 *September* 1987 *by M. Cardona*)

In selenium diffused, aluminium doped silicon a new electron paramagnetic resonance (EPR) spectrum, Si-NL31, was observed as a broad structure superposed on the selenium pair resonance. The EPR spectrum could not be analyzed directly, but an intense ^{27}Al electron nuclear double resonance (ENDOR) spectrum of trigonal symmetry was found to be related to it. The small hyperfine interaction combined with the large quadrupole effect are evidence for a negatively charged, substitutional Al acceptor, with a donor at the nearest neighbour position. By field scanned ENDOR the EPR spectrum could be analysed. The small anisotropy and shift of the *g*-value with respect to the free electron value is circumstantial evidence for the presence of a selenium double donor. The nearly vanishing contact density on the ^{27}Al nucleus is evidence for a doublet ground state, for which the defect axis lies in a nodal plane. This explains why the EPR spectrum shows no resolved ^{77}Se hyperfine structure. The connection to the infrared complex Si:Se(X_1), which also has a doublet groundstate, is discussed.

1. INTRODUCTION

CHALCOGEN CENTRES IN silicon have been extensively studied by electron paramagnetic resonance (EPR) [1–3] and ligand electron nuclear double resonance (ENDOR) [1, 4, 5]. A review of infrared (IR) absorption studies on chalcogens in silicon is given by Wagner *et al.* [6]. Chalcogen centres in silicon represent a theoretical challenge, as the effective mass theory describes the excited states very well, but fails for the ground states. They are also of technological interest, as Se is applied in infrared detectors [7] and S is a major contaminant in solar-grade silicon [8]. The isolated substitutional chalcogens and nearest neighbour substitutional chalcogen pairs show deep double donor behaviour and have been studied both in EPR (except for Te_2) and in IR absorption. Less well understood are the higher order chalcogen complexes reported from IR absorption studies [6, 9, 10]. The complexes designated X_1 and X_3 contain three chalcogens. For X_4 and X_5 the presence of two resp. one chalcogen has been demonstrated. Involvement of transition metals in these complexes is not likely, as was shown by intentional doping.

In this Communication a paramagnetic resonance study of a new chalcogen donor centre, hereafter referred to as Si-NL31, which incorporates a negatively charged acceptor, is presented. There is a close connection to the Se complex Se(X_1), which is a deep double donor [9, 10] and contributes to the infrared efficiency of Si:Se detectors [7].

2. EXPERIMENTAL

The sample was prepared by diffusion of Se into *p*-type floating-zone silicon doped with about 2×10^{16} Al atoms per cm^3 and a room temperature resistivity of 0.8 Ωcm. A 0.5 cm^3 quartz ampoule initially containing typically 1 mg of powdered Se mixed with excess Si powder and a $2 \times 2 \times 20$ mm^3 crystal was kept at 1370°C for a period of 5 days. Under these circumstances a 1 bar SiSe atmosphere is formed [11]. The ampoule volume was small to prevent deterioration of the crystal by vapour transport. After the diffusion treatment the ampoule was cooled down to room temperature in about 2 min. The magnetic resonance experiments were carried out on a K-band superheterodyne spectrometer operating at 23 GHz. The magnetic field was modulated at a frequency of 83 Hz. The nuclear magnetic resonance (NMR) signal for ENDOR measurements was chopped at a rate of 3.3 Hz. For a complete description see Sprenger [12]. The field scanned ENDOR (FSE) technique is extensively described by Niklas and Spaeth [13]. The usual procedure for ENDOR measurements is to lock the field on the EPR line while scanning the NMR fre-

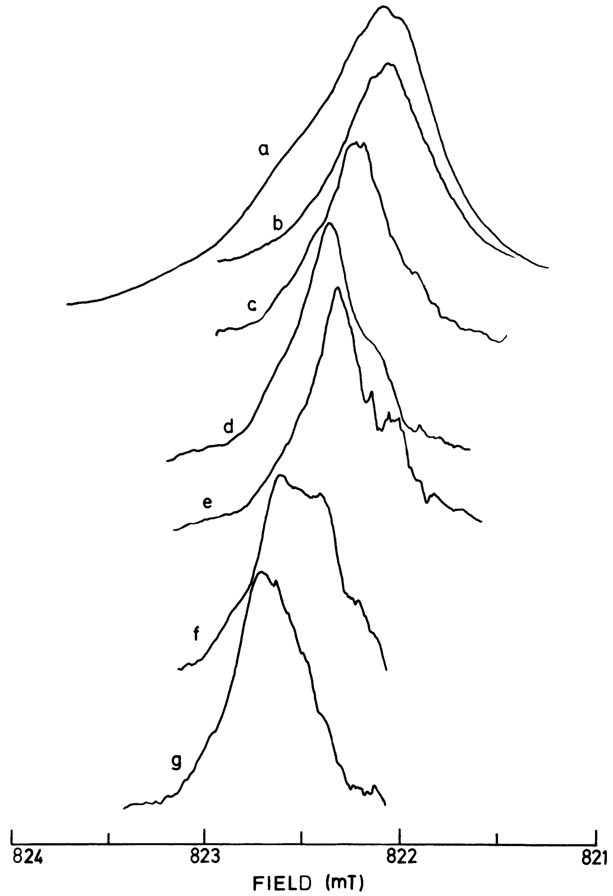

Fig. 1. The unravelling of the ESR spectrum with FSE for **B**||[1 0 0] at a microwave frequency of 23.036 GHz. (a) Central part of the total ESR spectrum. (b) A ^{29}Si FSE spectrum related to the Se_2^+ resonance. (c–g) The ^{27}Al FSE spectra of Si-NL31 for $m_S = 1/2$ and **B**||[1 0 0], showing the correlation to the structure on the high field flank of the Se_2^+ resonance. The transitions are (c) $[1/2, 3/2\rangle \leftrightarrow |1/2, 5/2\rangle$, (d) $|1/2, 1/2\rangle \leftrightarrow |1/2, 3/2\rangle$, (e) $|1/2, -1/2\rangle \leftrightarrow |1/2, 1/2\rangle$, (f) $|1/2, -3/2\rangle \leftrightarrow |1/2, -1/2\rangle$ and (g) $|1/2, -5/2\rangle \leftrightarrow |1/2, -3/2\rangle$.

quency, which produces an NMR-like spectrum. In FSE one locks the frequency to the NMR line and then scans the magnetic field. The observed ENDOR spectrum in this case looks like ordinary EPR, but only EPR transitions connecting levels involved in the NMR transition are observed. Thus FSE allows the study of unresolved EPR features.

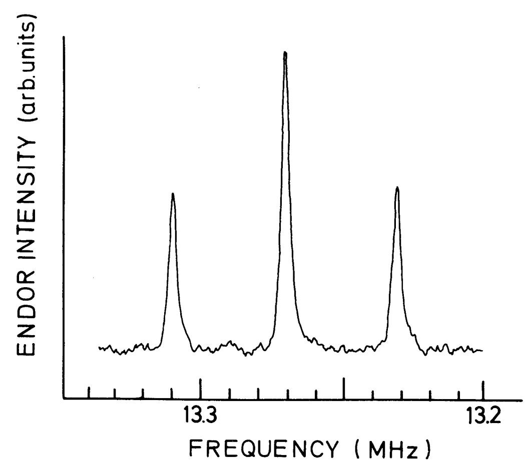

Fig. 2. Example of ^{27}Al ENDOR spectrum with **B**||[1 0 0]. Transition $|1/2, 3/2\rangle \leftrightarrow |1/2, 5/2\rangle$. The splitting in three lines with intensity ratio 1:2:1 is caused by a slight misalignment of the crystal.

3. RESULTS

In the temperature range from 10 to 15 K the well-known EPR spectra of Se^+ [2] and Se_2^+ [3] were detected with relative intensities of 1:2. These spectra are easily identified by the large, characteristic hyperfine interaction with the $I = 1/2$ nucleus of ^{77}Se (7.50% natural abundance). The predominance of the Se_2^+ resonance indicates a Fermi level between 306.5 meV (the $Se^{0/+}$ level) and 206.4 meV (the $Se_2^{+/++}$ level) below the conduction band [6]. The Se_2^+ resonance showed an asymmetric lineshape stemming from a broad featureless underlying EPR spectrum. From the intensity of the hyperfine structure, it was inferred that only 70% of the integrated intensity is due to Se_2^+. Part of the spectrum is shown in Fig. 1(a) for the magnetic field **B** parallel to the [1 0 0] direction. ENDOR measurements revealed intense, anisotropic resonances that were not related to the Se_2^+ resonance. In Fig. 2 an example of an ENDOR spectrum is shown. The very small linewidth of only 3 kHz enhances greatly the spectral resolution. It should be compared with the values of usually 100 kHz or more

Table 1. Observed spin Hamiltonian parameters for Si-NL31

Parameter	*xx*	*xy*	$\parallel$	$\perp$	
g	2.00106	0.00072	2.00250	2.00034	
g_N	11.0993				MHz/T
A	2.9046	1.8146	6.5338	1.0900	MHz
Q		0.5026	1.0052	−0.5026	MHz

encountered in the literature. FSE measurements showed the ENDOR spectrum to be related to the unresolved EPR structure. The FSE spectra for the various nuclear transitions with $m_S = +1/2$ and $\mathbf{B}\|[1\,0\,0]$ are shown in Fig. 1(c)–(g). For comparison, a ^{29}Si FSE spectrum related to Se_2^+ is shown in Fig. 1(b). The new centre is hereafter referred to as Si-NL31. The nuclear g-value was roughly determined by observing the shift of the ENDOR position as the magnetic field was varied within the EPR linewidth. A value of 10.5 ± 0.5 MHz/T was obtained, suggesting ^{27}Al as the nucleus responsible for the ENDOR. As the precise electron g-values of Si-NL31 could not be determined from the unresolved EPR, ENDOR and FSE measurements were performed simultaneously. The observed angular FSE patterns display trigonal symmetry. From the absence of multiple patterns, an electron spin $S = 1/2$ was deduced. The spectra could be described by the spin Hamiltonian

$$H = \mu_B \mathbf{B}\cdot\mathbf{g}\cdot\mathbf{S} - g_N\mu_N \mathbf{B}\cdot\mathbf{I} + \mathbf{S}\cdot\mathbf{A}\cdot\mathbf{I} + \mathbf{I}\cdot\mathbf{Q}\cdot\mathbf{I}, \qquad (1)$$

with nuclear spin $I = 5/2$. Because of the presence of strong ^{29}Si ENDOR, the nuclear spin could not be obtained directly from the multiplicity of the spectrum. A fit to within the linewidth of 3 kHz was obtained for the ENDOR spectrum, whereas the FSE resonances were observed within 10% of the 0.4 mT linewidth of the calculated positions. The resulting parameters are shown in Table 1.

The observed value of g_N is definite proof for the presence of the 100% abundant ^{27}Al nucleus, with $g_N = 11.094$ MHz/T [14]. The sign of g was assumed to be positive, as for a pure electron spin. Since g_N is known to be positive, A is expected to be also positive within the LCAO model discussed below. This experiment yields only the sign of the product $g \cdot g_N \cdot A \cdot Q$, which is determined to be positive. With the above assumptions, it then follows that $Q_{xy} > 0$. A computer simulation of the ^{27}Al ENDOR pattern is shown in Fig. 3. Its irregular appearance stems from the large quadrupole effect compared to the hyperfine interaction. Figure 4 gives the simulated EPR spectrum. In first order the quadrupole term does not influence the electronic transitions, but in higher order it leads to nonequidistant hyperfine splitting. The splittings are to be compared to the FSE linewidth of 0.4 mT.

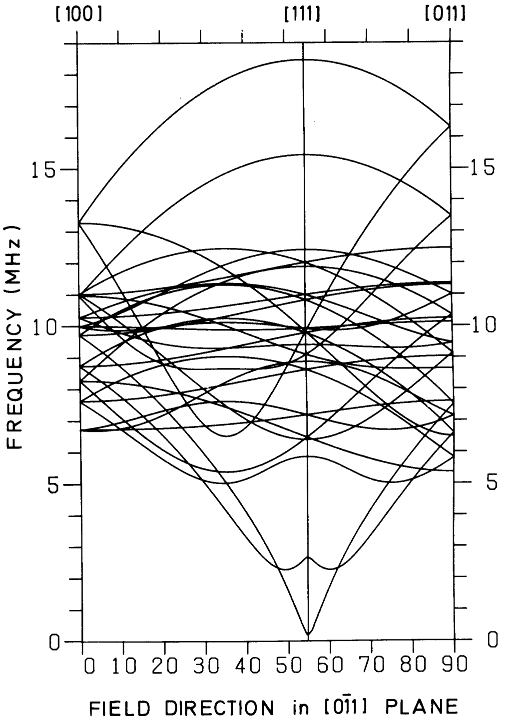

Fig. 3. Full angular dependence of the ^{27}Al ENDOR spectrum of Si-NL31, as calculated from the observed parameters at a microwave frequency of 23.043 GHz. The observed resonances were all situated within 3 kHz from the displayed curves.

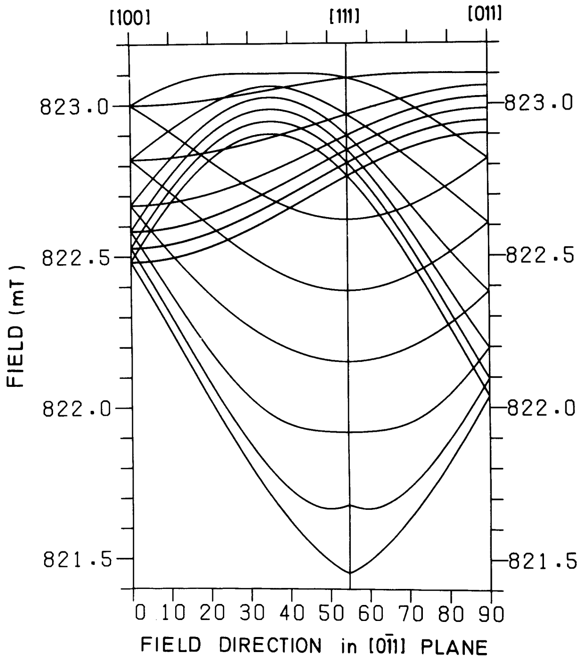

Fig. 4. Full angular dependence of the ESR spectrum of Si-NL31, as calculated from the observed parameters for a microwave frequency of 23.036 GHz. The deviations of the observed FSE positions from the displayed curves did not exceed 10% of the linewidth of 0.4 mT.

4. DISCUSSION

Starting from an LCAO interpretation of the observed nuclear interactions, it will now be argued that Si-NL31 consists of a nearest neighbour Al_s^- acceptor, paired to a Se_s^+ or incorporated in a $\mathrm{Se}^+(\mathrm{X}_1)$ double donor, which presumably has 3 Se atoms. Here the subscript s indicates a substitutional lattice site. The formation of such donor acceptor pairs is to be expected in view of the large Coulomb energy.

The ^{27}Al hyperfine interaction contains information about the unpaired spin density, that is, about the defect wave function. The defect wave function ψ is expanded in unpaired atomic orbitals ϕ_i situated at the lattice sites R_i

$$\psi = \sum_i \eta_i \phi_i . \tag{2}$$

For Al it is sufficient to take a combination of s and p orbitals

$$\phi = \alpha\phi_s + \beta\phi_p . \tag{3}$$

Throughout the following, the formulae given by Sprenger *et al.* [15] for the hyperfine and quadrupole interactions of s- and p-orbitals will be used without repeating them here. Following Morton and Preston [16], an Al s-orbital produces a contact interaction of $A = 3911\,\text{MHz}$ and, using g_N from Table 1, an Al p-orbital produces a hyperfine anisotropy of 83.1 MHz. Upon comparison with the observed values, one finds $\eta^2\alpha^2 = 0.075\%$ and $\eta^2\beta^2 = 2.18\%$. From the small value of $\eta^2\beta^2$ it follows that the Al atom is in a nonmagnetic charge state. Clearly another, paramagnetic, atom or complex must reside on the defect axis. The vanishingly small contact density indicates that the defect wave function has a node at the position of the ^{27}Al nucleus. The alternative that Al is at a distant site is clearly unattractive, in view of the large quadrupole interaction. The observed residual contact interaction may be due to core polarisation or to a small admixture of some excited state. Such an admixture can also explain the slight deviation from the free electron g-value. Of course, if A is interpreted as a residual effect, the above LCAO treatment is no longer valid. Then, also, A need no longer be positive and all that can be said is that A and Q have the same sign.

In contrast to the hyperfine interaction, the quadrupole interaction probes the charge distribution near the nucleus [17]. Though it contains contributions from nearby nuclear charges and defect electrons, it is dominated by deviations from tetrahedral symmetry of the valence electrons. Quadrupole interactions may therefore provide important clues to the structure of a defect. For a positive elementary point charge situated at 2.35 Å from a ^{27}Al nucleus along the [1 1 1] direction one obtains $q_{xy} = 20.0\,\text{kHz}$, using equation (12) of [15]. On the other hand, with equation (13) of [15], and [16], the unbalanced charge of a [1 1 1] oriented aluminium $3p$ orbital amounts to $q_{xy} = -1048\,\text{kHz}$. Using the observed value of $\eta^2\beta^2$, the fraction of the defect electron localized at the Al then contributes only $q_{xy} = -22.9\,\text{kHz}$. These constitute only small and opposite effects. The observed value of 502.6 kHz can only stem from axially distributed valence charges. From the LCAO analysis one obtains a charge imbalance of effectively 48.0% of a hole or electron along the defect axis. The possibility of an interstitial Al^+ with a pair of non-bonding p-orbitals oriented in the [1 1 1] plane cannot be ruled out, but the more likely configuration is substitutional Al_s^-. Support for this view comes from the $^{27}\text{Al}_s^-$ ENDOR spectrum of the Al_i^{++}–Al_s^- pair G19. This defect also has nearly free electron g-values [18] and a large quadrupole effect of 390 kHz with the Al_s^- nucleus [19]. The analysis of the quadrupole effect of Si-NL31 presented here, is, to our opinion, equally well applicable to G19. For Si-NL31 as well as G19, the large valence charge imbalance is evidence for a substantial trigonal lattice deformation at the Al site.

In order to arrive at a paramagnetic centre, the Al_s^- ion must be paired to a donor. The g-values are remarkably close to the free electron value, which excludes the involvement of a transition metal. The donor should be deep, so that the ground state is well separated in energy from other states, and no orbital momentum is mixed in through spin-orbit coupling with the conduction band [20]. The only known deep simple, non-transition metal donors are the interstitials Mg_i ($g = 1.9981$) [21], Al_i ($g = 2.0019$) [18], the vacancy ($1/3\text{tr}\{g\} = 2.0022$) [22] and chalcogen centres. Mg is a rather improbable unintended impurity and, furthermore, the $\text{Mg}_i^{+/++}$ level of 256.50 meV below the conduction band edge [23] is not deep enough, so that is g-value compares to the value of 1.9985 of the shallow group V donors. Al_i only forms upon irradiation and moreover, two trigonal Al_i^{++}–Al_s^- pairs, G19 and G20, are already known [18, 19]. Vacancy related complexes also form only upon irradiation and the known [17] trigonal defect AlV^- is also excluded. Since there is no alternative, we conclude to the involvement of the intentional dopant Se. The existence of a chalcogen acceptor complex was first proposed by Vydyanath *et al.* [24]. These authors report a reverse dependence on the boron concentration of the photoconductivity spectra of Se-diffused silicon, and conclude the formation of Se–B complexes. The 7.5% abundant ^{77}Se isotope with $I = 1/2$ should then give rise to hyperfne satellites. It will be argued below that the wave function is expected to have a node also on the donor position. In this case the hyperfine structure may be unresolved in EPR, whereas the low intensity ^{77}Se ENDOR may be obscured by the many ^{29}Si ENDOR resonances from Si-NL31, Se_2 and other defects that may be present.

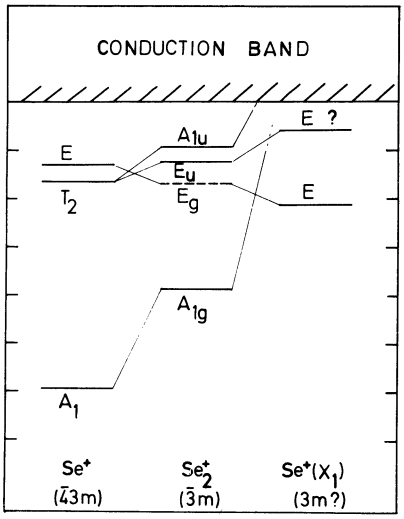

Fig. 5. Level scheme of 1*s* ground states of the ionised chalcogen centres Se^+ [6], Se_2^+ [6] and $Se^+(X_1)$ [9, 10]. The $1s(E)$ level of Se^+ was calculated by Altarelli [26]. The $1s(E_g)$ level is not known for Se_2^+, but was assumed to be situated below the $1s(E)$ level of Se^+, as for the neutral charge states.

The 1*s* ground states of chalcogen donors in Si can be written as

$$\psi(r) = \sum_{i=1}^{6} \alpha_i F_i(r)\phi_i(r), \tag{4}$$

where the F_i are envelope functions and the ϕ_i are the Bloch functions at the 6 equivalent conduction band minima. In the effective mass approximation F obeys a hydrogen-like equation and there is 6-fold degeneracy. A cubic central cell potential lifts the degeneracy and splits the ground state into a $1s(A_1)$ singlet, a $1s(E)$ doublet and a $1s(T_2)$ triplet. For a positive sign the singlet lies lowest, as shown in Fig. 5 for Se_s^+. If a trigonal potential is added, the $1s(T_2)$ level undergoes a further splitting into an odd $1s(A_{1u})$ singlet and an odd $1s(E_u)$ doublet state. For consistency, the even 1*s* states are renamed $1s(A_{1g})$ and $1s(E_g)$. The symmetry of these states is given below in symbolic form

$$\psi_{1s(A_{1g})} = x^2 + y^2 + z^2,$$

$$\psi_{1s(E_g)} = 2z^2 - x^2 - y^2, x^2 - y^2,$$

$$\psi_{1s(E_u)} = 2z - x - y, x - y,$$

$$\psi_{1s(A_{1u})} = x + y + z.$$

The states have distinct parity only if the centre has inversion symmetry. As shown in Fig. 5, the trigonal perturbation of the Se_2^+ pair (symmetry $\bar{3}m$) raises all levels, but lowers the $1s(E_g)$ level, as this level effectively avoids the trigonal axis. In a Se_s^+–Al_s^- donor-acceptor pair (symmetry $3m$) the trigonal potential would be even stronger and a $1s(E)$ level ends up lowest. This is consistent with the vanishing contact density on the ^{27}Al-nucleus and with the lack of resolved ^{77}Se hyperfine structure. One would expect the ground state, an orbital doublet occupied by a single electron, to be split by a Jahn–Teller deformation, and, consequently, to have lower than axial symmetry. As this is not observed, Si-NL31 should be a dynamical Jahn–Teller system. A similar conclusion is reached in a recent paper by Krag [25], reporting IR absorption measurements under applied stress on several sulphur centres. One centre, the trigonal double donor known as A or $S(X_1)$, in the neutral charge state showed splittings consistent with a doublet ground state. It is therefore tempting to identify Si-NL31 with the analogous $Se(X_1)$ complex [9]. Moreover, $Se(X_1)$ has a second ionisation level of 213.7 meV below the conduction band edge, which makes it the only known IR centre that is paramagnetic in the estimated range for the Fermi level of the crystal. In Fig. 5, also the 1*s* levels of the $Se^+(X_1)$ centre are shown. However, according to Wagner *et al.* [6], $Se(X_1)$ contains 3 chalcogens. ENDOR experiments on crystals doped with isotopically enriched Se are therefore needed to clarify the role of Se in Si-NL31.

In conclusion, the experimental evidence indicates a close relation between the new magnetic resonance centre Si-NL31 and the IR absorption centre $Se^+(X_1)$ and fully supports the assumption that both centres are manifestations of the same defect. Further research on the role of acceptors in chalcogen complexes may lead to a more complete understanding of these defects.

Acknowledgements — We thank Dr. A.A. Ezhevskii and P.G. Hettema for their assistance during the experiment, and also Dr. E.G. Sieverts for helpful comments. This work received financial support from the Foundation for Fundamental Research on Matter (FOM), The Netherlands.

REFERENCES

1. G.W. Ludwig, *Phys. Rev.* **137A,** 1520 (1965).
2. H.G. Grimmeiss, E. Janzén, H. Ennen, O.F. Schirmer, J. Schneider, R. Wörner, C. Holm, E. Sirtl & P. Wagner, *Phys. Rev.* **B24,** 4571 (1981).
3. R. Wörner & O.F. Schirmer, *Solid State Commun.* **51,** 665 (1984).
4. S. Greulich-Weber, J.R. Niklas & J.M. Spaeth, *J. Phys. C: Solid State Physics* **17,** L911 (1984).
5. J.R. Niklas & J.M. Spaeth, *Solid State Commun.* **46,** 121 (1983).

6. P. Wagner, C. Holm, E. Sirtl, R. Oeder & W. Zulehner, in, *Festkörperprobleme: Advances in Solid State Physics*, Vol XXIV, p. 191 (Edited by P. Grosse) Vieweg, Braunschweig, (1984).
7. N. Sclar, *J. Appl. Phys.* **52,** 5207 (1981).
8. J. Dietl, D. Helmreich & E. Sirtl, in, *Crystals: Growth, Properties and Applications Vol. 5*, Vol. 5, p. 43, Springer, Berlin, (1981).
9. J.C. Swartz, D.H. Lemmon & R.N. Thomas, *Solid State Commun.* **36,** 331 (1980).
10. E. Janzén, R. Stedman, G. Grossmann & H.G. Grimmeiss, *Phys. Rev.* **B29,** 1907 (1984).
11. C. Holm, *Thesis* (München, (1981)).
12. M. Sprenger, *Thesis* (Amsterdam, (1986)).
13. J.R. Niklas & J.M. Spaeth, *Phys. Status Solidi (b)* **101,** 221 (1980).
14. G.H. Fuller, *J. Phys. & Chem. Ref. Data* **5,** 835 (1976).
15. M. Sprenger, R. van Kemp, E.G. Sieverts and C.A.J. Ammerlaan, *Phys. Rev.* **B35,** 1582 (1987).
16. J.R. Morton & K.F. Preston, *J. Magn. Reson.* **30,** 577 (1978).
17. G.D. Watkins, *Phys. Rev.* **155,** 802 (1967).
18. G.D. Watkins, in *Radiation Damage in Semiconductors*, p. 97, Dunod, Paris, (1965).
19. J.R. Niklas, J.M. Spaeth & G.D. Watkins, *Mat. Res. Soc. Symp. Proc.* **46,** 237 (1985).
20. O.F. Schirmer & M. Scheffler, *J. Phys. C: Solid State Physics* **15,** L645 (1982).
21. J.E. Baxter & G. Ascarelli, *Phys. Rev.* **B7,** 2630 (1973).
22. G.D. Watkins, *J. Phys. Soc. Japan* **18,** Suppl. II, 22 (1963).
23. M. Kleverman, K. Bergman & H.G. Grimmeiss, *Semicond. Sci. Technol.* **1,** 49 (1986).
24. H.R. Vydyanath, J.S. Lorenzo & F.A. Kröger, *J. Appl. Phys.* **49,** 5928 (1978).
25. W.E. Krag, W.H. Kleiner & H.J. Zeiger, *Phys. Rev.* **B33,** 8304 (1986).
26. M. Altarelli, *Physica* **117B & 118B,** 122 (1983).